HHS Public Access

Author manuscript

Mamm Genome. Author manuscript; available in PMC 2017 January 13.

Published in final edited form as:

Mamm Genome. 2016 June ; 27(5-6): 179–190. doi:10.1007/s00335-016-9634-y.

Mouse genome-wide association study identifies polymorphisms on chromosomes 4, 11 and 15 for age-related cardiac fibrosis

Qiaoli Li[1,*], **Annerose Berndt**[2,3,*], **Beth A. Sundberg**[4], **Kathleen A. Silva**[4], **Victoria E. Kennedy**[4], **Clinton L Cario**[2], **Matthew A. Richardson**[2], **Thomas H. Chase**[4,†], **Paul N. Schofield**[4,5], **Jouni Uitto**[1], and **John P. Sundberg**[4]

[1]Department of Dermatology and Cutaneous Biology, Sidney Kimmel Medical College at Thomas Jefferson University, Philadelphia, PA 19107, USA

[2]Department of Medicine, University of Pittsburgh, Pittsburgh, PA 15261, USA

[3]University of Pittsburgh Medical Center, Pittsburgh, PA 15213, USA

[4]The Jackson Laboratory, Bar Harbor, ME 04609, USA

[5]Department of Physiology, Development and Neuroscience, University of Cambridge, Cambridge, UK

Abstract

Dystrophic cardiac calcinosis (DCC), also called epicardial and myocardial fibrosis and mineralization, has been detected in mice of a number of laboratory inbred strains, most commonly C3H/HeJ and DBA/2J. In previous mouse breeding studies between these DCC susceptible and the DCC resistant strain C57BL/6J, 4 genetic loci harboring genes involved in DCC inheritance were identified and subsequently termed *Dyscal* loci 1 through 4. Here we report susceptibility to cardiac fibrosis, a sub-phenotype of DCC, at 12 and 20 months of age and close to natural death in a survey of 28 inbred mouse strains. Eight strains showed cardiac fibrosis with highest frequency and severity in the moribund mice. Using genotype and phenotype information of the 28 investigated strains we performed genome-wide association studies (GWAS) and identified the most significant associations on chromosome (Chr) 15 at 72 million base pairs (Mb) ($P < 10^{-13}$) and Chr 4 at 122 Mb ($P < 10^{-11}$) and 134 Mb ($P < 10^{-7}$). At the Chr 15 locus *Col22a1* and *Kcnk9* were identified. Both have been reported to be morphologically and functionally important in the heart muscle. The strongest Chr 4 associations were located approximate 6 Mb away from the *Dyscal* 2 quantitative trait locus peak within the boundaries of the *Extl1* gene and in close proximity to the *Trim63* and *Cap1* genes. In addition, a single nucleotide polymorphism association was found on chromosome 11. This study provides evidence for more than the previously reported 4 genetic loci determining cardiac fibrosis and DCC. The study also highlights the power of GWAS in the mouse for dissecting complex genetic traits.

Corresponding author: Qiaoli Li, Ph.D., Department of Dermatology and Cutaneous Biology, Thomas Jefferson University, 233 South 10th Street, BLSB Building, Suite 431, Philadelphia, PA 19107, Tel: 215-503-5713; Fax: 215-503-5788, Qiaoli.Li@Jefferson.edu.

*Equal contribution

†Deceased

Keywords

Cardiac fibrosis; aging; dystrophic cardiac calcinosis (DCC); inbred strains of mice

Introduction

Dystrophic cardiac calcinosis (DCC), also known as epicardial and myocardial fibrosis and mineralization, has been reported for several inbred strains of mice, including C3H and DBA substrains, but not others, such as the most commonly used C57BL/6J mouse strain (Eaton et al. 1978; Firth and Ward 1988; Le Corre et al. 2012; Sundberg et al. 2014; Van Vleet and Ferrans 1987). This lesion has a variable presentation across many inbred strains in terms of severity, frequency, distribution, and ratio of fibrosis to mineralization. The most common presentation involves mineralization and fibrosis of the outermost layer of the right ventricular free wall of the heart, extending from the epicardium. The left ventricular free wall may also be involved but usually less severely. Focal lesions of various sizes may or may not occur throughout the myocardium. Crosses between C3H/HeJ and C57BL/6J mice identified 4 quantitative trait loci (QTL), designated as Dystrophic cardiac calcinosis 1 through 4 (*Dyscalc1-4*) (Ivandic et al. 2001). Similar studies were performed with DBA/2J and C57BL/6J crosses which identified similar genetic loci (Brunnert et al. 1999).

Mapping to mouse chromosome (Chr) 7 (Ivandic et al. 1996), *Dyscalc1* was associated with the ATP-binding cassette, sub-family C (CFTR/MRP), member 6 (*Abcc6*) gene (Aherrahrou et al. 2008; Meng et al. 2007). Mutations in this gene in humans and targeted genetic lesions in laboratory mice produce pseudoxanthoma elasticum (PXE), a multi-system disease manifesting with mineralization in the skin and vascular connective tissues (Li et al. 2016; Uitto et al. 2010). This observation in C3H substrains was extended to include the KK/HlJ and 129S1/SvImJ inbred strains in mouse aging studies, strains that have the same *Abcc6* allelic mutation (Berndt et al. 2013). Severe lesions in the KK/HlJ strain, closely resembling those seen in $Abcc6^{tm1Jfk}$ and $Abcc6^{tm1Aabb}$ genetically engineered null mice (Gorgels et al. 2005; Klement et al. 2005), suggest that KK/HlJ mice may be an alternative spontaneous mouse model for studying PXE (Li et al. 2012). By contrast, another inbred mouse strain, 129S1/SvImJ, carries the same *Abcc6* allelic polymorphism but does not exhibit most of the PXE-like lesions seen in KK/HlJ (Berndt et al. 2013), which raises the question of the percent of penetrance of the associated polymorphisms. Finally, additional modifier genes may be responsible for these phenotypic differences between strains.

As DCC has been considered a characteristic lesion for PXE in C3H and DBA substrains (strains with the same allelic mutations in their *Abcc6* gene) (Le Corre et al. 2012), examining heart lesions across 28 inbred strains provides an alternative approach to identification of modifier genes, such as those included within the *Dyscalc2-4* QTLs. Furthermore, while QTLs provide a genetic location in which to search for modifier genes, large scale, targeted mutant studies (knockout mice), in which the mutant mice have been carefully phenotyped histologically, provide additional candidates, especially when the mutant mice show features of mineralization similar to various degrees to that seen in the *Abcc6* null mice (phenotypic mimics). Such genes in mice include: family with sequence

similarity 20, member A and C (*Fam20a* and *Fam20c*) (Vogel et al. 2012), extracellular calcium-sensing receptor (*Casr*) (Hough et al. 2004), ectonucleotide pyrophosphatase/phosphodiesterase1 (*Enpp1*) (Li et al. 2014a; Li et al. 2013; Li et al. 2014b), klotho *(Kl)* (Hu et al. 2011), tripartite motif-containing 24 (*Trim24*; formerly transcription 1 alpha, *Tif1a*) (Ignat et al. 2008), and others (Kornak 2011; Li and Uitto 2013). These may be primary genes responsible for the phenotype or they may be integrated into one or more molecular pathways. Finally, single nucleotide polymorphisms (SNP) analyses, combined with literature review, can be an effective way to identify and begin to validate candidate genes.

While there is currently no single genetic approach to identify all the genes that induce, regulate progression, and ultimately cause lesions in various diseases, each method provides pieces of this complicated puzzle. Routine QTL mapping of F2 progeny for all traits of a disease generally results in large genetic intervals but identification of specific genes is often not successful, as was shown for various models of inflammatory bowel disease (Beckwith et al. 2005; Birkenmeier et al. 1995; Bristol et al. 2000; Farmer et al. 2001; Mahler et al. 1998; Mahler et al. 1999). However, combining QTL mapping with analysis of sub-congenic mouse lines for lymphatic changes in inflammatory bowel disease resulted in the identification and validation of the specific genes responsible for that trait (Jurisic et al. 2010). An alternative approach to those described above is to use the genetic and phenotypic diversity among a large number of inbred strains in genome-wide association studies (GWAS). These unbiased population studies have been useful to identify genome variations responsible for airway hyper-responsiveness and pulmonary adenomas (Berndt et al. 2011a; Berndt et al. 2011b; Leme et al. 2010).

Here we performed population analysis for cardiac fibrosis in aged mice of 28 strains and identified novel candidate genes using a plethora of bioinformatics technologies, including GWAS. Genes identified are involved in initiation of disease to its ultimate outcome and severity indicating that these combined approaches can refine the molecular pathogenesis of cardiac fibrosis and serve as a template to similar investigations of other diseases.

Materials and methods

Mice

Aging study—Mice were obtained from a large-scale aging study performed at the Jackson Aging Center that has been described in detail elsewhere (Sundberg et al. 2011). The following 31 strains were examined in this present study: 129S1/SvImJ, A/J, AKR/J, BALB/cByJ, BTBRT^{+}*tf*/J, BUB/BnJ, C3H/HeJ, C57BL/10J, C57BL/6J, C57BLKS/J, C57BR/cdJ, C57L/J, CAST/EiJ, CBA/J, DBA/2J, FVB/NJ, KK/HIJ, LP/J, MRL/MpJ, NOD.B10Sn-H2^{b}/J (a congenic strain with the NOD genetic background but with a histocompatibility locus from a diabetes-resistant strain), NON/ShiLtJ, NZO/HlLtJ, NZW/LacJ, P/J, PL/J, PWD/PhJ, RIIIS/J, SJL/J, SM/J, SWR/J, and WSB/J. Three of the strains were not evaluated because of lymphoma development (AKR/J), lack of enough mice for analysis (CAST/EiJ), and self-mutilations resulting in euthanasia for humane purposes (SJL/J) (Sundberg et al. 2011). Therefore, analyses were performed in 28 strains of mice. Mice from several cross-sectional cohorts (at 12 and 20 months) and a longitudinal (close to natural death) cohort were evaluated for heart lesions. Fifteen females and 15 males for each

strain entered the cross-sectional cohorts and 65 females and 35 males entered the longitudinal study group. Cross-sectional and longitudinal groups were set-up in parallel. Those mice that survived were euthanized by CO_2 asphyxiation, weighed, and underwent complete necropsies at the defined ages (Silva and Sundberg 2012).

Retired breeders—Ten female and 10 male mice were obtained from The Jackson Laboratory (Bar Harbor, ME) as retired breeders (*i.e.*, 5–10 months of age depending on the rotation time for the colony)(Flurky et al. 2009) from the following 16 inbred strains: A/J, BALB/cByJ, BALB/cJ, C3H/HeJ, C57BL/6J, C57BL/10J, C57BR/cdJ, C57L/J, DBA/2J, FVB/NJ, KK/HlJ, LP/J, PWD/PhJ, SWR/J, MRL/MpJ-*Fas*^{lpr}/J, and SJL/J. Mice were euthanized by CO_2 asphyxiation, weighed, and the hearts were removed and processed for histologic evaluation.

All protocols were reviewed and approved by The Jackson Laboratory Animal Care and Use Committee. Mouse handling and care were followed according to the Public Health Service animal welfare policies using IACUC approved methods.

Tissue fixation and preparation

Hearts in the aging study and retired breeder study were removed and fixed in Fekete's acid-alcohol-formalin solution for 12 hours then transferred to 70% ethanol, trimmed (in the four chamber longitudinal orientation), and processed routinely for histology. One and sometimes two serial sections were stained with hematoxylin and eosin (H&E). For the retired breeder study at least two hearts were sectioned in the four chamber longitudinal orientation (bisected, two sections per heart, two sets per slide) whereas the remainder were sectioned transversely at the equator, base, and apex (3 sections per heart, two sets per slide) (Chase et al. 2009). A third slide was stained with Masson's Trichrome only for hearts obtained from retired breeders.

Quantification of lesion severity

Histology slides were reviewed by an experienced, board-certified veterinary pathologist (John P. Sundberg). Histological diagnosis of cardiac fibrosis was evaluated per strain and gender. The frequency and degree of epicardial mineralization and fibrosis, ventricular free wall atrophy, and ventricular fibrosis of the left and right heart were evaluated separately. The inter-ventricular septum and myocardium was also reviewed for lesions. The severity is based on a subjective measure of the size of the lesion (scores: 0 - normal; 1 - mild; 2 - moderate; 3 - severe; 4 - extreme). Selected cases were photographed to document the range in severity and are available on Pathbase (http://www.pathbase.net/). Cardiac fibrosis was also defined by frequency (percentage of mice diagnosed with cardiac fibrosis per total number of mice per strain and gender). Data were recorded and coded using the Mouse Disease Information System (MoDis) (Sundberg et al. 2008).

Histology

Diagnosis of heart lesions, while evident at the time of necropsy, was confirmed by histopathology and graded based on extent and distribution. A number of the commonly used inbred strains, notably DBA/2J, C3H/HeJ, BALB/cJ, and BALB/cByJ, had various

combinations of epicardial mineralization and fibrosis (primarily but not exclusively on the right ventricular free wall), which can also be scattered through the myocardium, a disease commonly referred to as DCC (Frith and Ward 1988). Whether the mineralization was the initiating event or a sequela to the fibrosis was not determined. However, ectopic mineralization, which can involve multiple other organs (Berndt et al. 2012), appears to be controlled by a number of other genes that complicate genetic interpretation of the mechanisms. As such, these processes were separated and fibrosis, independent of mineralization, was the focus of this investigation.

Genome-wide association mapping and variant identification

Phenotype-genotype association analysis was performed using the expedited efficient mixed-model association (EMMAX) algorithm (Kang et al. 2010). Frequencies and mean severities of the fibrosis phenotype in 28 strains of mice were used as input phenotype data. Four million SNPs (available at http://mouse.cs.ucla.edu/mousehapmap/full.html) were used as input genotype data. Each SNP was evaluated individually and recorded as −log(*P*-values) as the strength of the genotype-phenotype associations and graphically displayed in Manhattan plots. SNP effects were determined using the Variant Effect Predictor tool by Ensembl (http://useast.ensembl.org/info/docs/tools/vep/index.html). Coding region SNPs known to change the amino acid sequence (*i.e.*, non-synonymous SNPs) were tested for functional importance using the PolyPhen-2 algorithm (http://genetics.bwh.harvard.edu/pph2/) (Adzhubei et al. 2010).

Statistical analysis

Frequencies and strain means ± SEM of phenotype severities were calculated separately for each age group by genders using JMP8 statistical analysis software (https://www.jmp.com/software/jmp8/). Fisher's exact test was used to determine the difference in frequencies and the two-sided Kruskal-Wallis nonparametric test was used to determine the differences in severity between males and females for each strain. The Kruskal-Wallis test is comparable to one-way analysis of variance, but without the parametric assumptions. All statistical computations were completed using SPSS version 15.0 software (SPSS Inc., Chicago, IL).

Results and discussion

Cardiac fibrosis datasets - aging survey and retired breeders

We had two independent datasets for age-related cardiac fibrosis phenotype in different strains of mice. The first was an aging study which was divided into a longitudinal or life span investigation (65 females and 35 males each strain) and a cross-sectional study (15 females and 15 males each strain), to evaluate onset and diversity of diseases at 12 and 20 months of age on 28 inbred strains of mice. Mice in the longitudinal study were allowed to become moribund at which point they were euthanized by CO_2 asphyxiation. All investigated strains were part of a large-scale aging study by the Jackson Aging Center which has been described in detail elsewhere (Sundberg et al. 2011). The second study was performed on mice of 16 inbred strains as retired breeders from the production facilities of The Jackson Laboratory. They are the retired mice at 5–10 months of age (10 females and 10 males each strain) depending on the rotation time for the colony. Cardiac tissues were

collected and prepared from all the mice described above for histopathology for cardiac lesions. For detailed description of these two datasets, see Materials and methods section under “Mice”.

Histology

Cardiac fibrosis varied in severity and distribution between individuals and between strains with increasing fibrosis frequency and severity in older mice (Fig. 1). In general, cardiac fibrosis was diagnosed in the left and right ventricular wall, inter-ventricular septum, and myocardium to various degrees in inbred mouse strains (Frith and Ward 1988). These lesions are described in detail in mouse pathology textbooks (Frith and Ward 1988; Mohr et al. 1996) and many additional images from this study can be found online (http://www.pathbase.net/) (Schofield et al. 2010).

The C57BL/10J strain has rarely been associated with heart lesions in the literature (Neu et al. 1987), yet these mice had severe fibrosis of the right ventricular free wall usually, but not exclusively, without mineralization associated with severe atrophy of the cardiac muscle. Masson’s Trichrome staining illustrated increased collagen deposition in hearts from C57BL/10J at 10 months of age compared to C57BL/6J at 8 months of age, which had little except around vessels as would be expected (Fig. 2). Retrospective review of our computerized medical records of disease surveillance in all strains since 1987 revealed that these heart changes, particularly the severe right ventricular fibrosis and atrophy, have been a feature of C57BL/10J since the time these records were collected.

Frequency and severity of cardiac fibrosis

Among the 28 mouse strains of the aging study, 8 strains (A/J, BALB/cByJ, C3H/HeJ, C57BL/10J, DBA/2J, KK/HlJ, NZO/H1LtJ and PL/J) developed cardiac fibrosis at different stages of the entire aging process (Table S1). While five strains (A/J, BALB/cByJ, C57BL/10J, DBA/2J and KK/HlJ) were affected in the 12 month group, 7 strains were affected in the 20 month group and in moribund mice. Most frequently, lesions were observed in moribund mice that were close to natural death of all strains (Table 1). Similarly, the severity of the lesions was strongest in the moribund mice of all strains (Table 2).

Mice from the 16 retired breeder strains were obtained at 5 to 10 months of age. Mice of 7 strains (A/J, BALB/cByJ, BALB/cJ, C3H/HeJ, C57BL/10J, DBA/2J and KK/HlJ) developed cardiac fibrosis (Table S2). C57BL/10J and DBA/2J mice had the highest severity scores among 16 retired breeder strains (Table 3). BALB/cByJ had a higher frequency of heart lesions than its closely related substrain, BALB/cJ.

Genome-wide association mapping for cardiac fibrosis frequency and severity

GWAS has been proven successful to identify causative genomic loci for a number of disease phenotypes. GWAS analysis excels traditional QTL studies because it utilizes denser SNP panels for identification of smaller genomic regions, which leads to fewer candidate genes for subsequent experimental verification. As part of the large-scale ageing study at the Jackson Ageing Center, 28 inbred mouse strains at 12 and 20 months of age develop various degrees of fibrosis in the heart, with respect to both frequency and severity. The large scale

phenotype dataset and various degrees of phenotype allow us to identify genes associated with cardiac fibrosis frequency and severity by GWAS analysis.

Phenotype-genotype association analysis was performed using the expedited efficient mixed-model association (EMMAX) algorithm (Kang et al. 2010). Frequencies (for affected strains: Table 1) and mean severities (for affected strains: Table 2) of the fibrosis phenotype in 28 strains of mice were used as input phenotype data. Phenotypes from males and females were combined to increase the power for the genetic analysis. Four million SNPs were used as input genotype data.

For the 12 month age group, strong associations with frequency ($P = 1.1 \times 10^{-11}$) and severity ($P = 1.5 \times 10^{-10}$) of cardiac fibrosis were found on Chr 4 at 122,602,996 base pairs (bp) (Fig. 3A, frequency; Fig. 3B, severity). There were also strong associations on Chr 11 at 3,614,390 bp (frequency: $P = 8.6 \times 10^{-9}$; severity: $P = 8.6 \times 10^{-11}$) and 46,911,030 bp (frequency: $P = 1.2 \times 10^{-8}$; severity: $P = 1.3 \times 10^{-10}$). While the region on Chr 4 was supported by 4 adjacent SNP associations, each locus on Chr 11 was a single SNP association.

For the 20 month age group, left ventricular fibrosis was associated most significantly with frequency ($P = 9.9 \times 10^{-11}$) and severity ($P = 5.5 \times 10^{-13}$) on Chr 15 at 72,274,700 bp (Fig. 3C, frequency; Fig. 3D, severity). The Chrs 4 and 11 associations shown for the 12 month age group could also be detected in this 20 month age group; however, they were less significant. For frequency, the Chr 4 association had a *P*-value of 1.2×10^{-5} and the Chr 11 association at 3,614,390 bp showed a *P*-value of 5.5×10^{-6}. For severity, the strongest Chr 4 association was no longer located at about 122.6 million base pairs (Mb) but at 134.4 Mb with as many as 12 SNPs in close proximity ($P = 8.6 \times 10^{-7}$). The Chr 11 associations at about 3.6 and 46.9 Mb showed *P*-values of 9.2×10^{-6} and 9.8×10^{-6}, respectively.

Identification of candidate genes

GWAS identified several new genome locations that potentially point to novel biomarkers determining the phenotypic variations in cardiac fibrosis. The phenotype-genotype association on Chr 4 at about 122.6 Mb was located about 5 Mb proximal of the *Dyscalc* 2 QTL peak at 127.8 Mb. Cyclase-associated protein 1 (*Cap1*) is located 250 Kb downstream of this SNP association. Interestingly, a recent investigation showed that the lack of *Cap1*'s isoform *Cap2* leads to dilated cardiomyopathy (Peche et al. 2013). The Chr 4 association at about 134.4 Mb was located within close proximity of the *Dyscalc* 2 QTL peak. The SNP association was found to be located within the boundaries of the gene exostoses (multiple)-like 1 (*Extl1*). Some rare variants of multiple exostoses are associated with cardiomyopathy in humans (Atiq and Aziz 1997; Hamouda et al. 2011).

Two other genes, solute carrier family 30 (zinc transporter), member 2 (*Slc30a2*) and tripartite motif-containing 63 (*Trim63*), are located approximately at 20 kb and 45 kb, respectively, upstream of the SNP associations and the gene platelet-activating factor acetylhydrolase 2 (*Pafah2*) is located about 21 kb downstream. Interestingly, *Trim63* has been associated with several human heart conditions, such as hypertrophic cardiomyopathy,

chronic heart failure and aging metabolism, and cardiac ischemia/reperfusion injury (Chen et al. 2012).

The phenotype-genotype association on Chr 15 at about 72.3 Mb is located about 400 kb upstream of collagen, type XXII, alpha 1 (*Col22a1*) and about 240 kb downstream of potassium channel, subfamily K, member 9 (*Kcnk9*, formerly *Task3*). *Col22a1* is a part of tissue junctions and commonly found in skeletal and heart muscles (Koch et al. 2004). In addition, this was a noted candidate gene for isoproterenol induced cardiac fibrosis in a young mouse model (Rau et al. 2015). Immununofluorescence screening revealed that COL22A1 protein was expressed at the chordae tendineae insertion sites into the muscle of the right ventricle in adult C57BL/6J mice (data not shown), consistent with the tissue junction expression of this protein in postnatal mouse tissues, as previously reported (Koch et al. 2004). *Kcnk9* is differentially expressed in developing hearts where it contributes to the potassium conductance that is responsible for cardiac excitability (Kim et al. 2000).

In a massive histopathological screening of all organ systems in 28 inbred strains of mice of both genders (Sundberg et al. 2011), dystrophic cardiac calcinosis was diagnosed in 8 strains. Within the affected mice, a subgroup had areas of fibrosis without mineralization. Lesions varied in severity and location within the hearts between the strains. Genome-wide association mapping of cardiac fibrosis determined that none of the QTLs previously identified for DCC, in which mineralization is a major feature, corresponded to any identified loci. The same was true for fibro-osseous lesions, another pathological process found in strains that exhibit mineralization and fibrotic lesions in bones and other organs (*e.g.*, skin) including C3H/HeJ (Berndt et al. 2016).

While it is relatively easy to see clinical correlations between seemingly unrelated diseases with small numbers of mice undergoing experimental manipulation, it is critically important to understand strain-specific background lesions before drawing conclusions. The mineralization phenomena among inbred strains are very complicated. Some of the phenotypic observations are related to each other due to shared genetic predispositions. However, the underlying genetic basis can be modified by genes involved in other diseases which add to the complexity of the predisposition. Such appears to be the case for *Abcc6* and ectopic mineralization (Berndt et al. 2013). There have been correlations to a specific SNP in the *Abcc6* gene in C3H/HeJ, DBA/2J, and KK/HlJ mice that get ectopic mineralization and DCC and in 129S1/SvImJ, which gets ectopic mineralization but not the heart lesions (Berndt et al. 2013). However, BALB/cJ, BALB/cByJ, C57BL/10J and A/J also develop these heart lesions, but do not exhibit this genomic variation in *Abcc6*. Therefore, these results suggest that *Abcc6* is rather a modifier gene for the complex PXE phenotype and not the primary cause of heart lesions. Evaluation of the Sanger mouse SNP database (http://www.sanger.ac.uk/cgi-bin/modelorgs/mousegenomes/snps.pl) reveals that A/J and BALB/cByJ have three non-synonymous coding SNPs in *Abcc6*, which are not found in the other strains (positions at 53,232,273 bp, 53,232,660 bp, and 53,274,055 bp). These SNPs presumably could have an effect on the phenotype thereby suggesting that these mice are additional models for PXE. The organ specificity observed for the mineralization/fibrosis syndrome may potentially represent individual diseases altogether due to the complex genetic background of each trait as shown here.

In a mouse cardiac ischemia-reperfusion model, investigators found that genetically engineered C57BL/6 mice with a null mutation in *Abcc6* had larger infarcts than wild type controls. Conversely, transgenic mice expressing wildtype *Abcc6* in C3H/HeJ, which are naturally hypomorphic for *Abcc6*, had reduced infarct size compared to C3H/HeJ mice without the transgene suggesting that ABCC6 was a novel modulator of cardiac myocyte survival after injury (Mungrue et al. 2011). A study using 23 inbred mouse strains using beta-adrenergic cardiac blockade or stimulation found a great deal of variability between the strains (Berthonneche et al. 2009). Another study utilized over 100 inbred and recombinant inbred strains, including 25 of the 28 studied here. Female mice, 8–10 weeks of age were treated with isoproterenol (ISO) for 21 days (total age 11–13 weeks) and hearts evaluated for cardiac fibrosis and mineralization. Mice in this induced model had GWAS performed and while they found over 24 candidate loci, each containing an average of 14 genes, they focused on *Abcc6*. Using targeted *Abcc6* mutant and KK/HlJ mice they concluded that "the age-associated calcification phenotype observed in *Abcc6* KO is distinct from the ISO-induced cardiac fibrosis phenotype" (Rau et al. 2015). These findings confirm that *Abcc6* is involved with some aspects of myocardial health and response to injury and aging, but it is one of many genes and not likely, in and of itself, to be the primary cause of DCC. They also note *Col22a1* as a highlighted gene, one of 6 in the ISO treated fibrosis intervals on Chr 15 (Rau et al. 2015). *Col22a1* was a major candidate gene in the study reported here for age associated cardiac fibrosis suggesting this protein may play an important role in myocardial fibrosis induced by a variety of different types of insults to the heart.

Non-synonymous SNPs in the *Abcc6* gene are considered to account for the *Dyscalc1* QTL (Aherrahrou et al. 2008; Meng et al. 2007). Although 5 Mb distal, *Dyscalc2* may involve identified variants in *Cap1*, *Extl1*, *Slc20a2*, *Pafah2*, but especially *Trim63* as this gene is associated with some types of heart disease (Chen et al. 2012). No candidate genes were identified in this GWAS to account for the *Dyscalc3* or *4* QTLs. However, *Col22a1* and *Kcnk9* on Chr 15 appear to be important and demonstrate that when many strains are evaluated it is possible to find new genes (or at least genomic regions) while losing significance for others presumably because of dilution of the signal through the broader genomic variety when performing strain surveys compared to two strain QTL crosses. This and many other complex genetic traits have to be evaluated by many approaches, such as crosses between inbred strains in the earliest studies (Brunnert et al. 1999; Ivandic et al. 2001), GWAS analyses for as many strains as possible (as in the current studies), to large scale targeted mutagenesis of genes for which little is currently known, as was done by the Lexicon phenotyping program (Hough et al. 2004; Schofield et al. 2012; Vogel et al. 2012) or as is currently being done in the KOMP2 project (Brown et al. 2007; DiTommaso et al. 2015). There is no single approach to address all aspects of a complex genetic disease. Furthermore, comparing and contrasting similar diseases between species, as with humans and mice in this case, combined with new discoveries on the genetics and pathophysiology will continue to unravel the complexities of many common diseases that affect all mammalian species.

Supplementary Material

Refer to Web version on PubMed Central for supplementary material.

Acknowledgments

The authors thank Jesse Hammer and Josiah Raddar for technical assistance.

Research reported in this publication was supported by the Ellison Medical Foundation, Parker B. Francis Foundation, and the National Institutes of Health (R01AR055225 and K01AR064766). Mouse colonies were supported by the National Institutes of Health under Award Number AG25707 for the Jackson Aging Center. The content is solely the responsibility of the authors and does not necessarily represent the official views of the National Institutes of Health. The Jackson Laboratory Shared Scientific Services were supported in part by a Basic Cancer Center Core Grant from the National Cancer Institute (CA34196).

Abbreviations

Abcc6	ATP-binding cassette, sub-family C(CRTR/MRP), member 6 gene
Cap1	cyclase-associated protein 1 gene
Cap2	CAP, adenylate cyclase-associated protein 2 (yeast)
Col22a1	collagen, type XXII, alpha1
DCC	dystrophic cardiac calcinosis
Dyscalc1-4	dystrophic cardiac calcinosis 1–4 quantitative trait loci
EMMAX	expedited efficient mixed-model association
Extl1	exostoses (multiple)-like 1 gene
Fam20a/Fam20c	family with sequence similarity 20 member A and C genes
GWAS	genome-wide association studies
ISO	isoproterenol
Kcnk9	potassium channel, sub-family K, member 9 gene
Kl	klotho gene
MoDis	Mouse Disease Information System (MoDis)
Pafah2	platelet-activating factor acetylhydrolase 2 gene
PXE	pseudoxanthoma elasticum
QTL	quantitative trait locus
Slc30a2	solute carrier family 30 (zinc transporter), member 2 gene
Trim24	tripartite motif-containing 24 (formerly *Tif1a*)
Trim63	tripartite motif-containing 63

References

Adzhubei IA, Schmidt S, Peshkin L, Ramensky VE, Gerasimova A, Bork P, Kondrashov AS, Sunyaev SR. A method and server for predicting damaging missense mutations. Nat Methods. 2010; 7:248–249. [PubMed: 20354512]

Aherrahrou Z, Doehring LC, Ehlers EM, Liptau H, Depping R, Linsel-Nitschke P, Kaczmarek PM, Erdmann J, Schunkert H. An alternative splice variant in *Abcc6*, the gene causing dystrophic calcification, leads to protein deficiency in C3H/He mice. J Biol Chem. 2008; 283:7608–7615. [PubMed: 18201967]

Atiq M, Aziz K. Familial progressive cardiac conduction disorder and multiple exostoses. J Pak Med Assoc. 1997; 47:169–172. [PubMed: 9301171]

Beckwith J, Cong Y, Sundberg JP, Elson CO, Leiter EH. Cdcs1, a major colitogenic locus in mice, regulates innate and adaptive immune response to enteric bacterial antigens. Gastroenterology. 2005; 129:1473–1484. [PubMed: 16285949]

Berndt A, Ackert-Bicknell C, Silva KA, Kennedy VE, Sundberg BA, Cates JM, Schofield PN, Sundberg JP. Genetic determinants of fibro-osseous lesions in aged inbred mice. Exp Mol Pathol. 2016; 100:92–100. [PubMed: 26589134]

Berndt A, Cario CL, Silva KA, Kennedy VE, Harrison DE, Paigen B, Sundberg JP. Identification of *Fat4* and *Tsc22d1* as novel candidate genes for spontaneous pulmonary adenomas. Cancer Res. 2011a; 71:5779–5791. [PubMed: 21764761]

Berndt A, Leme AS, Williams LK, Von Smith R, Savage HS, Stearns TM, Tsaih SW, Shapiro SD, Peters LL, Paigen B, Svenson KL. Comparison of unrestrained plethysmography and forced oscillation for identifying genetic variability of airway responsiveness in inbred mice. Physiol Genomics. 2011b; 43:1–11. [PubMed: 20823217]

Berndt A, Li Q, Potter C, Liang Y, Silva KA, Kennedy V, Yuan R, Uitto J, Sundberg JP. A single nucleotide polymorphism in the *Abcc6* gene associates with connective tissue mineralization in mice similar to targeted models for pseudoxanthoma elasticum. J Invest Dermatol. 2012; 133:833–836. [PubMed: 23014343]

Berndt A, Li Q, Potter CS, Liang Y, Silva KA, Kennedy V, Uitto J, Sundberg JP. A single-nucleotide polymorphism in the Abcc6 gene associates with connective tissue mineralization in mice similar to targeted models for pseudoxanthoma elasticum. J Invest Dermatol. 2013; 133:833–836. [PubMed: 23014343]

Berthonneche C, Peter B, Schupfer F, Hayoz P, Kutalik Z, Abriel H, Pedrazzini T, Beckmann JS, Bergmann S, Maurer F. Cardiovascular response to beta-adrenergic blockade or activation in 23 inbred mouse strains. PLoS One. 2009; 4:e6610. [PubMed: 19672458]

Birkenmeier, E.; Torrey, A.; Sundberg, J. Chromosomal location of modifier genes determining sensitivity of mice to dextran sulphate sodium. In: Tytgat, G.; Bartelsman, J.; Deventer, SV., editors. Falk Symposium. Vol. 85. Den Haag: Kluwer Academic Publishers; 1995. p. 401-407.

Bristol IJ, Farmer MA, Cong Y, Zheng XX, Strom TB, Elson CO, Sundberg JP, Leiter EH. Heritable susceptibility for colitis in mice induced by IL-10 deficiency. Inflamm Bowel Dis. 2000; 6:290–302. [PubMed: 11149562]

Brown SJ, Tilli CM, Jackson B, Avilion AA, MacLeod MC, Maltais LJ, Lovering RC, Byrne C. Rodent Lce gene clusters; new nomenclature, gene organization, and divergence of human and rodent genes. J Invest Dermatol. 2007; 127:1782–1786. [PubMed: 17410201]

Brunnert SR, Shi S, Chang B. Chromosomal localization of the loci responsible for dystrophic cardiac calcinosis in DBA/2 mice. Genomics. 1999; 59:105–107. [PubMed: 10395807]

Chase TH, Cox GA, Burzenski L, Foreman O, Shultz LD. Dysferlin deficiency and the development of cardiomyopathy in a mouse model of limb-girdle muscular dystrophy 2B. Am J Pathol. 2009; 175:2299–2308. [PubMed: 19875504]

Chen SN, Czernuszewicz G, Tan Y, Lombardi R, Jin J, Willerson JT, Marian AJ. Human molecular genetic and functional studies identify TRIM63, encoding Muscle RING Finger Protein 1, as a novel gene for human hypertrophic cardiomyopathy. Circ Res. 2012; 111:907–919. [PubMed: 22821932]

DiTommaso T, Jones L, Cottle DL, Program WMG, Gerdin AK, Vancollie VE, Watt FM, Ramirez-Solis R, Bradley A, Steel KP, Sundberg JP, White JK, Smyth IM. Identification of genes important for cutaneous function revealed by a large scale reverse genetic screen in the mouse. PLoS Genet. 2015:10.

Eaton GJ, Custer RP, Johnson FN, Stabenow KT. Dystrophic cardiac calcinosis in mice: genetic, hormonal, and dietary influences. Am J Pathol. 1978; 90:173–186. [PubMed: 145807]

Farmer MA, Sundberg JP, Bristol IJ, Churchill GA, Li R, Elson CO, Leiter EH. A major quantitative trait locus on chromosome 3 controls colitis severity in IL-10-deficient mice. Proc Natl Acad Sci U S A. 2001; 98:13820–13825. [PubMed: 11707574]

Firth, CH.; Ward, JM. Color atlas of neoplastic and non-neoplastic lesions in aging mice. Amsterdam: Elsevier; 1988.

Flurky, K.; Currer, J.; Leiter, EH.; Witham, B. The Jackson Laboratory Handbook on Genetically Standardized Mice. Laboratory, TJ., editor. Bar Harbor; 2009.

Frith, CH.; Ward, JM. Color atlas of neoplastic and non-neoplastic lesions in aging mice. Amsterdam: Elsevier; 1988.

Gorgels TG, Hu X, Scheffer GL, van der Wal AC, Toonstra J, de Jong PT, van Kuppevelt TH, Levelt CN, de Wolf A, Loves WJ, Scheper RJ, Peek R, Bergen AA. Disruption of *Abcc6* in the mouse: novel insight in the pathogenesis of pseudoxanthoma elasticum. Hum Mol Genet. 2005; 14:1763–1773. [PubMed: 15888484]

Hamouda HI, Abulhasan S, Al-awadi S. Hereditary multiple exostoses, macrocephaly, congenital heart disease, developmental delay, and mental retardation in a female patient: A possible new syndrome? Or new association? Egyptian J Med Hum Genet. 2011; 12:95–98.

Hough TA, Bogani D, Cheeseman MT, Favor J, Nesbit MA, Thakker RV, Lyon MF. Activating calcium-sensing receptor mutation in the mouse is associated with cataracts and ectopic calcification. Proc Natl Acad Sci U S A. 2004; 101:13566–13571. [PubMed: 15347804]

Hu MC, Shi M, Zhang J, Quinones H, Griffith C, Kuro-o M, Moe OW. Klotho deficiency causes vascular calcification in chronic kidney disease. J Am Soc Nephrol. 2011; 22:124–136. [PubMed: 21115613]

Ignat M, Teletin M, Tisserand J, Khetchoumian K, Dennefeld C, Chambon P, Losson R, Mark M. Arterial calcifications and increased expression of vitamin D receptor targets in mice lacking TIF1alpha. Proc Natl Acad Sci U S A. 2008; 105:2598–2603. [PubMed: 18287084]

Ivandic BT, Qiao JH, Machleder D, Liao F, Drake TA, Lusis AJ. A locus on chromosome 7 determines myocardial cell necrosis and calcification (dystrophic cardiac calcinosis) in mice. Proc Natl Acad Sci U S A. 1996; 93:5483–5488. [PubMed: 8643601]

Ivandic BT, Utz HF, Kaczmarek PM, Aherrahrou Z, Axtner SB, Klepsch C, Lusis AJ, Katus HA. New *Dyscalc* loci for myocardial cell necrosis and calcification (dystrophic cardiac calcinosis) in mice. Physiol Genomics. 2001; 6:137–144. [PubMed: 11526197]

Jurisic G, Sundberg JP, Bleich A, Leiter EH, Broman KW, Buechler G, Alley L, Vestweber D, Detmar M. Quantitative lymphatic vessel trait analysis suggests Vcam1 as candidate modifier gene of inflammatory bowel disease. Genes Immun. 2010; 11:219–231. [PubMed: 20220769]

Kang HM, Sul JH, Service SK, Zaitlen NA, Kong SY, Freimer NB, Sabatti C, Eskin E. Variance component model to account for sample structure in genome-wide association studies. Nat Genet. 2010; 42:348–354. [PubMed: 20208533]

Kim Y, Bang H, Kim D. TASK-3, a new member of the tandem pore K(+) channel family. J Biol Chem. 2000; 275:9340–9347. [PubMed: 10734076]

Klement JF, Matsuzaki Y, Jiang QJ, Terlizzi J, Choi HY, Fujimoto N, Li K, Pulkkinen L, Birk DE, Sundberg JP, Uitto J. Targeted ablation of the *Abcc6* gene results in ectopic mineralization of connective tissues. Mol Cell Biol. 2005; 25:8299–8310. [PubMed: 16135817]

Koch M, Schulze J, Hansen U, Ashwodt T, Keene DR, Brunken WJ, Burgeson RE, Bruckner P, Bruckner-Tuderman L. A novel marker of tissue junctions, collagen XXII. J Biol Chem. 2004; 279:22514–22521. [PubMed: 15016833]

Kornak U. Animal models with pathological mineralization phenotypes. Joint Bone Spine. 2011; 78:561–567. [PubMed: 21550285]

Le Corre Y, Le Saux O, Froeliger F, Libouban H, Kauffenstein G, Willoteaux S, Leftheriotis G, Martin L. Quantification of the calcification phenotype of *Abcc6*-deficient mice with microcomputed tomography. Am J Pathol. 2012; 180:2208–2213. [PubMed: 22469843]

Leme AS, Berndt A, Williams LK, Tsaih SW, Szatkiewicz JP, Verdugo R, Paigen B, Shapiro SD. A survey of airway responsiveness in 36 inbred mouse strains facilitates gene mapping studies and identification of quantitative trait loci. Mol Genet Genomics. 2010; 283:317–326. [PubMed: 20143096]

Li Q, Aranyi T, Varadi A, Terry SF, Uitto J. Research progress in pseudoxanthoma elasticum and related ectopic mineralization disorders. J Invest Dermatol. 2016; 136:550–556. [PubMed: 26902123]

Li Q, Berndt A, Guo H, Sundberg J, Uitto J. A novel animal model for pseudoxanthoma elasticum - the KK/HlJ mouse. Am J Pathol. 2012; 181:1190–1196. [PubMed: 22846719]

Li Q, Chou DW, Price TP, Sundberg JP, Uitto J. Genetic modulation of nephrocalcinosis in mouse models of ectopic mineralization: the Abcc6(tm1Jfk) and Enpp1(asj) mutant mice. Lab Invest. 2014a; 94:623–632. [PubMed: 24732453]

Li Q, Guo H, Chou DW, Berndt A, Sundberg JP, Uitto J. Mutant *Enpp1*^{asj} mouse as a model for generalized arterial calcification of infancy. Dis Model Mech. 2013; 6:1227–1235. [PubMed: 23798568]

Li Q, Pratt CH, Dionne LA, Fairfield H, Karst SY, Sundberg JP, Uitto J. Spontaneous *asj-2J* mutant mouse as a model for generalized arterial calcification of infancy: A large deletion/insertion mutation in the *Enpp1* gene. PLoS One. 2014b; 9:e113542. [PubMed: 25479107]

Li Q, Uitto J. Mineralization/anti-mineralization networks in the skin and vascular connective tissues. Am J Pathol. 2013; 183:10–18. [PubMed: 23665350]

Mahler M, Bristol IJ, Leiter EH, Workman AE, Birkenmeier EH, Elson CO, Sundberg JP. Differential susceptibility of inbred mouse strains to dextran sulfate sodium-induced colitis. Am J Physiol. 1998; 274:G544–551. [PubMed: 9530156]

Mahler M, Bristol IJ, Sundberg JP, Churchill GA, Birkenmeier EH, Elson CO, Leiter EH. Genetic analysis of susceptibility to dextran sulfate sodium-induced colitis in mice. Genomics. 1999; 55:147–156. [PubMed: 9933561]

Meng H, Vera I, Che N, Wang X, Wang SS, Ingram-Drake L, Schadt EE, Drake TA, Lusis AJ. Identification of *Abcc6* as the major causal gene for dystrophic cardiac calcification in mice through integrative genomics. Proc Nat Acad Sci USA. 2007; 104:4530–4535. [PubMed: 17360558]

Mohr, U.; Dungworth, DL.; Capen, CC.; Carlton, WW.; Sundberg, JP.; Ward, JM. Intl Life Sciences Institute. Pathobiology of the aging mouse. Washington, DC: 1996.

Mungrue IN, Zhao P, Yao Y, Meng H, Rau C, Havel JV, Gorgels TG, Bergen AA, MacLellan WR, Drake TA, Bostrom KI, Lusis AJ. *Abcc6* deficiency causes increased infarct size and apoptosis in a mouse cardiac ischemia-reperfusion model. Arterioscler Thromb Vasc Biol. 2011; 31:2806–2812. [PubMed: 21979437]

Neu N, Rose NR, Beisel KW, Herskowitz A, Gurri-Glass G, Craig SW. Cardiac myosin induces myocarditis in genetically predisposed mice. J Immunol. 1987; 139:3630–3636. [PubMed: 3680946]

Peche VS, Holak TA, Burgute BD, Kosmas K, Kale SP, Wunderlich FT, Elhamine F, Stehle R, Pfitzer G, Nohroudi K, Addicks K, Stockigt F, Schrickel JW, Gallinger J, Schleicher M, Noegel AA. Ablation of cyclase-associated protein 2 (CAP2) leads to cardiomyopathy. Cell Mol Life Sci. 2013; 70:527–543. [PubMed: 22945801]

Rau CD, Wang J, Avetisyan R, Romay MC, Martin L, Ren S, Wang Y, Lusis AJ. Mapping genetic contributions to cardiac pathology induced by Beta-adrenergic stimulation in mice. Circ Cardiovasc Genet. 2015; 8:40–49. [PubMed: 25480693]

Schofield PN, Gruenberger M, Sundberg JP. Pathbase and the MPATH ontology. Community resources for mouse histopathology. Vet Pathol. 2010; 47:1016–1020. [PubMed: 20587689]

Schofield PN, Vogel P, Gkoutos GV, Sundberg JP. Exploring the elephant: histopathology in high-throughput phenotyping of mutant mice. Dis Model Mech. 2012; 5:19–25. [PubMed: 22028326]

Silva, KA.; Sundberg, JP. Necropsy methods. In: Hedrich, HJ., editor. The Laboratory Mouse. London: Academic Press; 2012. p. 779-806.

Sundberg JP, Berndt A, Sundberg BA, Silva KA, Kennedy V, Bronson R, Yuan R, Paigen B, Harrison D, Schofield PN. The mouse as a model for understanding chronic diseases of aging: The histopathologic basis of aging in inbred mice. Pathobiol Aging Age Relat Dis. 2011; 1:7179.doi: 10.3402/pba.V1i0.7179

Sundberg JP, Chevallier L, Silva KA, Kennedy VE, Sundberg BA, Li Q, Uitto J, King LE Jr, Berndt A. Mouse alopecia areata and heart disease: know your mouse! J Invest Dermatol. 2014; 134:279–281. [PubMed: 23774530]

Sundberg JP, Sundberg BA, Schofield P. Integrating mouse anatomy and pathology ontologies into a phenotyping database: tools for data capture and training. Mamm Genome. 2008; 19:413–419. [PubMed: 18797968]

Uitto J, Li Q, Jiang Q. Pseudoxanthoma elasticum: molecular genetics and putative pathomechanisms. J Invest Dermatol. 2010; 130:661–670. [PubMed: 20032990]

Van Vleet JF, Ferrans VJ. Ultrastructural changes in inherited cardiac calcinosis of DBA/2 mice. Am J Vet Res. 1987; 48:255–261. [PubMed: 3826865]

Vogel P, Hansen GM, Read RW, Vance RB, Thiel M, Liu J, Wronski TJ, Smith DD, Jeter-Jones S, Brommage R. Amelogenesis imperfecta and other biomineralization defects in Fam20a and Fam20c null mice. Vet Pathol. 2012; 49:998–1017. [PubMed: 22732358]

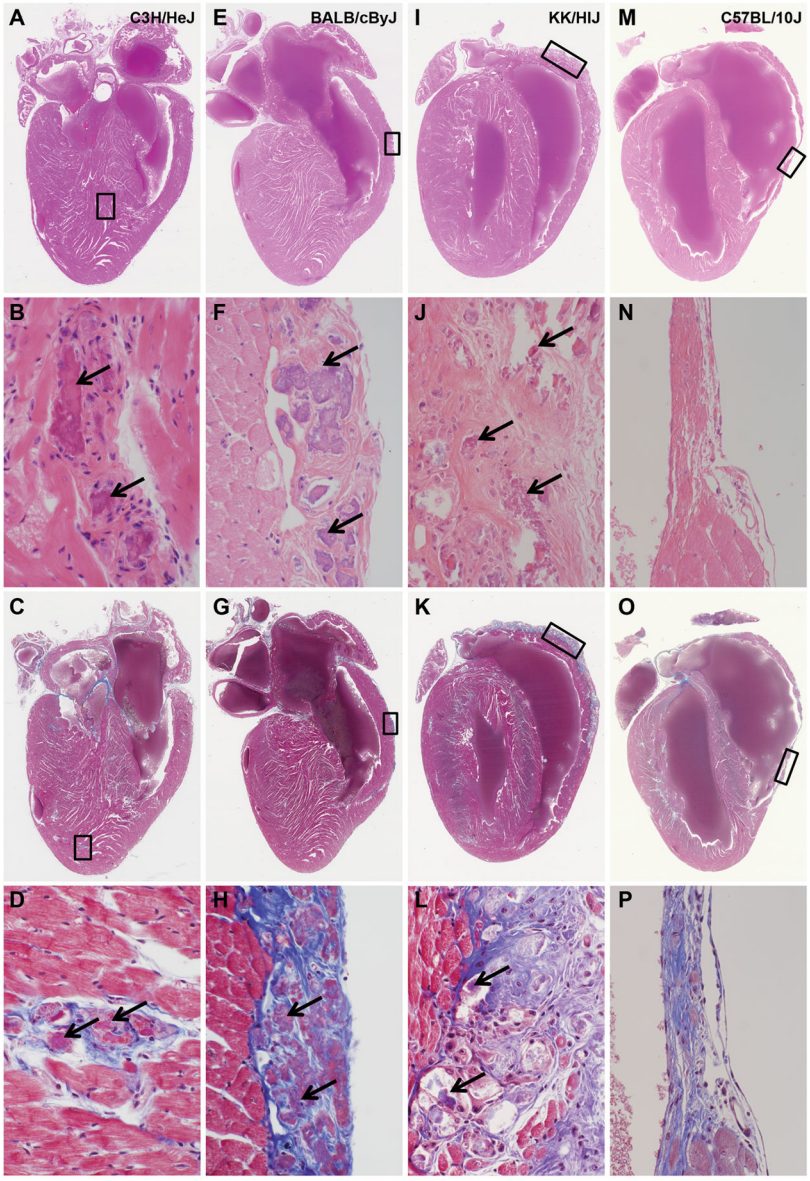

Figure 1. Heart lesions among inbred strains of mice

Focal myocardial fibrosis and mineralization (A–D, C3H/HeJ), right ventricular wall epicardial mineralization and fibrosis (E–H, BALB/cByJ; I–L, KK/HlJ), and right and left ventricular wall atrophy and fibrosis (M–P, C57BL/10J) represent the variety of changes observed in the heart. Arrows indicate areas of mineralization. The top two rows have hearts are stained with hematoxylin and eosin (H&E). The second row is a series of enlargements of the boxed areas in image above it. The bottom two rows are stained with Masson's Trichrome to label collagen deposition (blue stained areas).

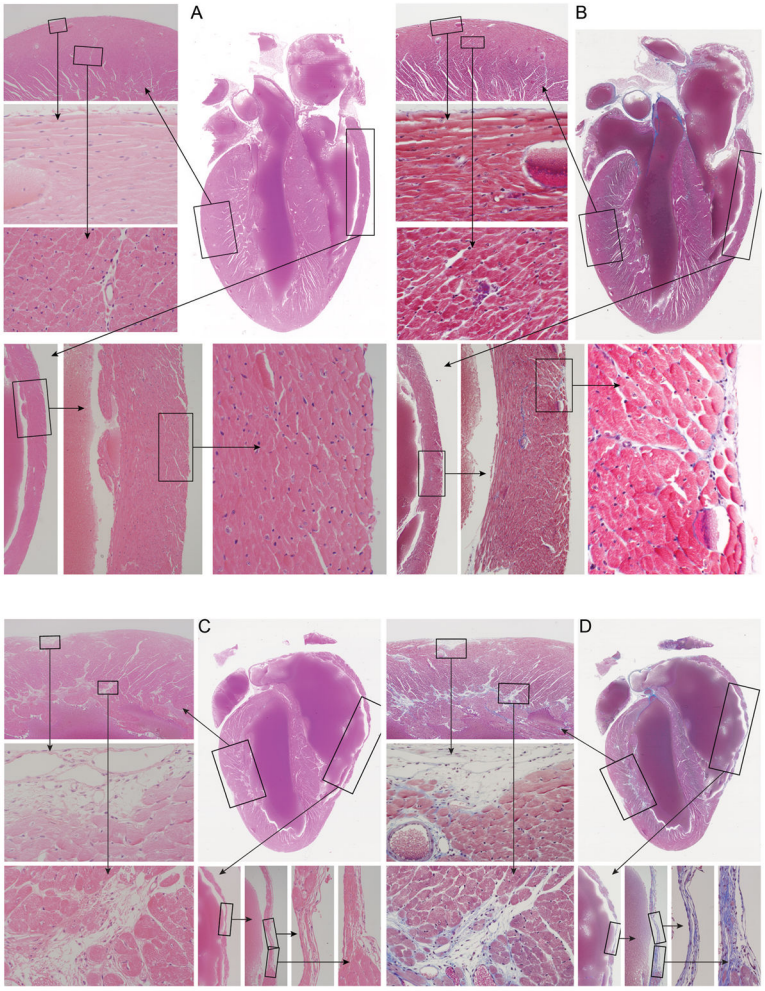

Figure 2. Comparison of hearts in female C57BL6/J and C57BL/10J mice 8 and 10 months of age, respectively

The top panel (C57BL/6J; A, H&E; B, Masson's Trichrome) is a normal heart with a small focus of mineralization in the left ventricle in the Masson's stained section. Boxed areas are enlarged as indicated with arrows for detail. The lower panel (C57BL/10J; C, H&E; D, Masson's Trichrome) reveals severe cardiac fibrosis primarily in the right ventricular wall but also throughout the left ventricle. Trichrome staining shows increased collagen deposition (blue stained areas). The right ventricular wall is completely replaced by fibrous connective tissue in multiple areas.

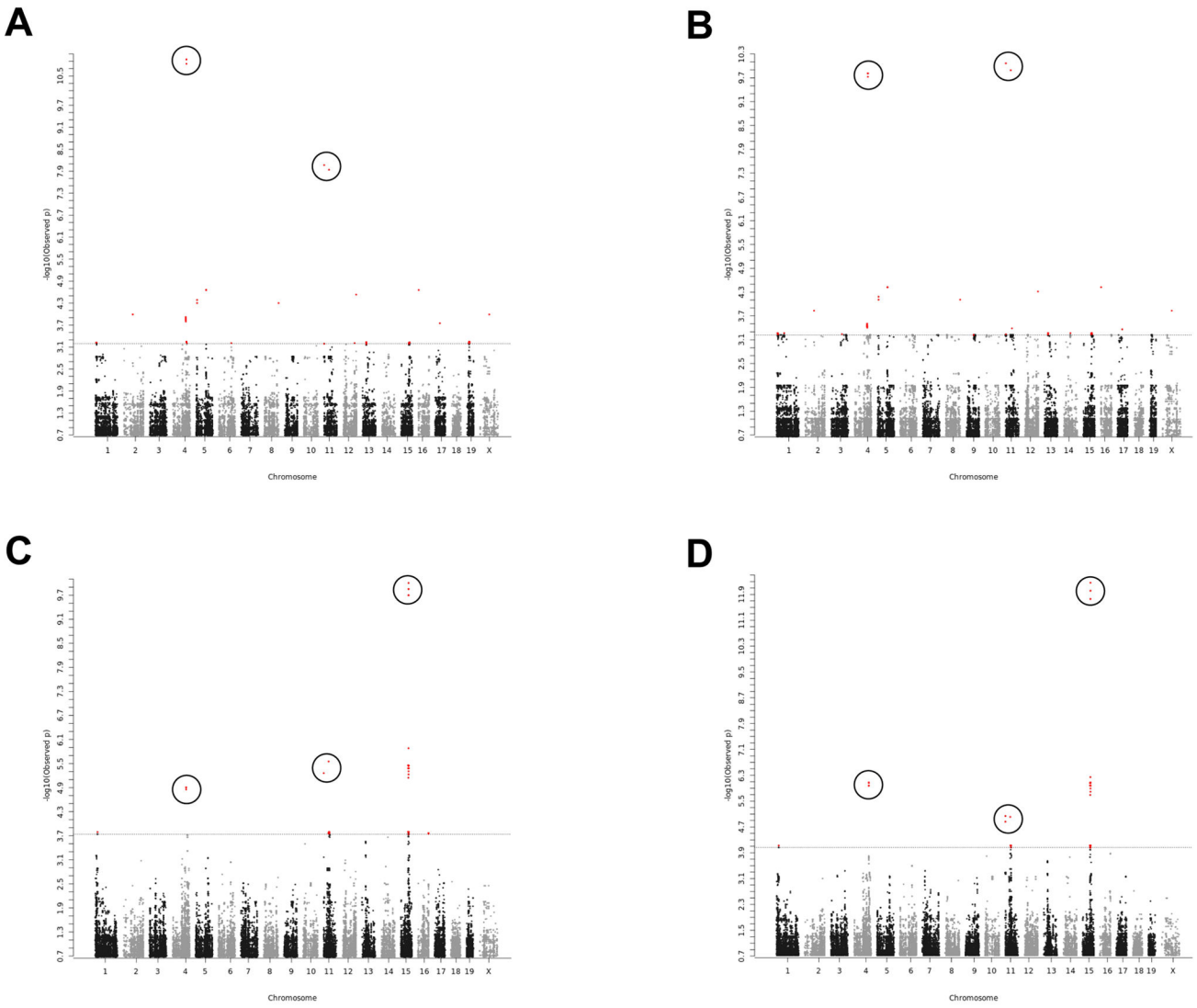

Figure 3. Genome-wide association scan for frequency (A) and severity (B) of cardiac fibrosis in 12 month old mice, and for frequency (C) and severity (D) of cardiac fibrosis in 20 month old mice

The SNPs with the highest Lod scores in chromosomes 4, 11 and 15 are indicated by circling.

Table 1

Frequency of cardiac fibrosis phenotype in 8 affected strains of mice in the aging study

Affected strains	12 mo		20 mo		Moribund	
	F	M	F	M	F	M
A/J	3/14 (21.4)	2/13 (15.4)	4/7 (57.1)	1/9 (11.1)	15/19 (78.9)	5/10 (50.0)
BALB/cByJ	2/14 (14.3)	3/14 (21.4)	5/15 (33.3)	6/9 (66.7)	6/12 (50.0)	3/4 (75.0)
C3H/HeJ	0/9 (0)	0/14 (0)	0/6 (0)	1/10 (10.0)	2/13 (15.4)	2/5 (40.0)
C57BL/10J	3/14 (21.4)	4/14 (28.6)	7/12 (58.3)	5/14 (35.7)	2/4 (50.0)	4/7 (57.1)
DBA/2J	10/12 (83.3)	10/11 (90.9)	4/7 (57.1)	5/6 (83.3)	5/5 (100.0)	6/7 (85.7)
KK/HlJ	11/15 (73.3)	9/12 (75.0)	6/7 (85.7)	3/7 (42.9)	2/4 (50.0)	2/3 (66.7)
NZO/HlLtJ	0/12 (0)	0/5 (0)	0/6 (0)	1/5 (20.0)	NA	0/2 (0)
PL/J	0/9 (0)	0/14 (0)	0/5 (0)	0/2 (0)	1/1 (100.0)	0/1 (0)

NA, no mice were examined for the strain. F, female; M, male.

Values were expressed as the number of affected mice by the total number of mice, and the percent of affected animals per strain and gender.

Table 2

Severity of cardiac fibrosis phenotype in 8 affected strains of mice in the aging study

Affected strains	12 mo		20 mo		Moribund	
	F	M	F	M	F	M
A/J	0.43±0.25	0.23±0.17	0.71±0.29	0.10±0.11 *	1.58±0.25	0.80±0.33
BALB/cByJ	0.36±0.25	0.21±0.11	1.00±0.39	1.89±0.51	1.17±0.42	1.75±0.85
C3H/HeJ	0	0	0	0.10±0.11	0.15±0.15	0.60±0.40
C57BL/10J	0.64±0.34	0.50±0.25	1.17±0.32	0.71±0.30	0.50±0.29	1.43±0.69
DBA/2J	3.00±0.43	3.36±0.36	0.57±0.20	2.67±0.67 **	3.40±0.25	3.14±0.63
KK/HlJ	2.13±0.41	1.42±0.36	2.29±0.61	0.86±0.46	1.50±0.96	1.00±0.58
NZO/HlLtJ	0	0	0	0.40±0.40	NA	0
PL/J	0	0	0	0	2.00	0

The scoring of cardiac fibrosis was based on a subjective measure of the size of the lesion by an experienced, board-certified veterinary pathologist (JPS). NA, no mice were examined for the strain. F, female; M, male.

Severity of scores: 0, normal; 1, mild; 2, moderate; 3, severe; 4, extreme. Values were expressed as mean score ± SEM.

* $P < 0.05$,

** $P < 0.01$ *vs.* females for the same strain at the same age.

Table 3

Frequency and severity of cardiac fibrosis phenotype in 7 affected retired breeder strains of mice

Affected strains	Frequency		Severity	
	F	M	F	M
A/J	6/10 (60.0)	2/10 (20.0)	1.20±0.36	0.20±0.13 *
BALB/cByJ	8/10 (80.0)	8/10 (80.0)	1.40±0.31	1.80±0.39
BALB/cJ	5/10 (50.0)	3/10 (30.0)	0.50±0.17	0.30±0.15
C3H/HeJ	10/10 (100.0)	6/10 (60.0)	1.50±0.22	1.20±0.39
C57BL/10J	10/10 (100.0)	10/10 (100.0)	2.90±0.18	2.60±0.22
DBA/2J	10/10 (100.0)	8/10 (80.0)	3.00±0.33	2.00±0.39
KK/HlJ	10/10 (100.0)	8/10 (80.0)	2.50±0.34	1.40±0.34 *

The frequency of cardiac fibrosis was expressed as the number of affected mice by the total number of mice and percent of affected animals. The scoring of cardiac fibrosis was based on a subjective measure of the size of the lesion by an experienced, board-certified veterinary pathologist (JPS). Severity of scores were expressed as mean score ± SEM. 0, normal; 1, mild; 2, moderate; 3, severe; 4, extreme. F, female; M, male.

* $P < 0.05$ vs. females for the same strain.